



ELSEVIER

Global and Planetary Change 35 (2002) 1–23

GLOBAL AND PLANETARY
CHANGE

www.elsevier.com/locate/gloplacha

Variations in tree cover in North America since the last glacial maximum

John W. Williams*

National Center for Ecological Analysis and Synthesis, University of California, Santa Barbara, CA 93101, USA

Abstract

Accurate reconstructions of late-Quaternary land-cover change are needed to better understand past interactions of the terrestrial biosphere with other components of the earth system. This paper presents a sequence of reconstructed needleleaved and broadleaved tree-cover densities for North America since the last glacial maximum, generated from fossil-pollen data and present-day tree-cover estimates derived from the Advanced Very High Resolution Radiometer (AVHRR). For this study, a refined form of the modern analog technique was developed, called the hierarchical analog technique, which can constrain paleoenvironmental properties even for fossil-pollen assemblages without close analogs in the modern-pollen record. Pollen taxa from samples that are compositionally unlike any modern-pollen samples are regrouped into plant functional categories based upon phenology, life form, leaf shape, and climatic tolerances, and the analog analysis rerun. Reclassifying individual pollen taxa into broader functional categories enables analogs to be found when no compositional analogs exist, but at a cost of increased uncertainties in the analog estimates. Tests of the hierarchical analog technique shows that it accurately reconstructs present-day tree-cover densities. The median standard deviation for each individual estimate is <10%. Tree-cover densities during the last glacial maximum were low relative to present, and have increased since. Lower-than-present tree-cover densities at the last glacial maximum were likely due to a combination of low temperatures, low precipitation, and low atmospheric CO₂ concentrations. By 14 ka, broadleaved tree-cover densities had begun to rise in the southeastern US and needleleaved forests grew in the western US, southeastern US, and as a belt along the southern margin of the Laurentide Ice Sheet. By the mid-Holocene, the northern and western needleleaved forests had joined. Needleleaved and broadleaved tree densities continued to increase until European settlement. Mapping percent tree-cover represents a useful alternative to biome-based classification schemes, enabling a fuller representation of vegetational gradients in space and time, and can be directly compared to the tree distributions simulated by dynamic global vegetation models. In effect, by calibrating the modern-pollen data against the AVHRR-derived estimates of tree-cover, the fossil-pollen data are applied to extrapolate satellite-based observations into the Quaternary, enabling study of vegetation dynamics and land-cover change at timescales beyond the period of direct observation by engineered remote sensors. Analog-based approaches, however, require extensive networks of surface and fossil-pollen samples, making further data collection a priority in sparsely sampled regions of the world.

© 2002 Elsevier Science B.V. All rights reserved.

Keywords: AVHRR; biogeography; land-cover; pollen; remote sensing; quaternary; vegetation

* Tel.: +1-805-892-2513; fax: +1-805-892-2510.

E-mail address: williams@nceas.ucsb.edu (J.W. Williams).

1. Introduction

Land-cover change at continental scales is forced by variations in climate, atmospheric CO₂, and human activity. In turn, terrestrial ecosystem dynamics are an important modulator of regional climates and atmospheric composition (Pielke et al., 1998). Vegetation influences such physical properties of the land surface as albedo and roughness length, as well as the fluxes of water, carbon, and energy between the vegetation and atmosphere (Rind, 1984; Sellers et al., 1997; Pielke et al., 1998). Land-cover change has affected the amount of carbon sequestered in the terrestrial biosphere, both recently (Houghton, 2001) and since the last glacial maximum (Crowley, 1995; Adams and Faure, 1998).

The distribution of individual plant taxa and biomes has changed dramatically since the last glacial maximum, primarily in response to climatic changes induced by variations in the earth's orbit. Sensitivity experiments with prescribed vegetation and general circulation models (Foley et al., 1994; Kutzbach et al., 1996; Broström et al., 1998) and coupled vegetation–atmosphere models suggest that the different land-cover configurations of the past are likely to have modified late-Quaternary climates (de Noblet et al., 1996; Texier et al., 1997; Ganopolski et al., 1998a,b; Kubatzki and Claussen, 1998; Levis et al., 1999). Accurate evaluation of the impacts of past vegetational change requires high-quality data-based reconstructions of the vegetation (Prentice and Webb, 1998).

Most of the information about late-Quaternary vegetation comes from fossil-pollen records archived in unlithified lake and mire sediments. Spatially explicit analyses of fossil-pollen datasets have shown that plant populations responded independently to late-Quaternary environmental change (Davis, 1976; Huntley and Birks, 1983; Thompson, 1988; Webb, 1988), from which higher-order properties of the vegetation emerge (Prentice and Webb, 1998; Williams et al., *in preparation*). Previous reconstructions of late-Quaternary land-cover have categorized past vegetation into a limited number of cover types, or biomes (Overpeck et al., 1992; Prentice and Webb, 1998 and references therein). Such reconstructions are useful when comparing with modern vegetation maps (Küchler, 1964; Matthews, 1983; Olson et al., 1984;

DeFries et al., 1998; Loveland et al., 2000) and vegetation representations within biogeochemistry and biogeography models (e.g. Prentice et al., 1992; Hunt et al., 1996). Describing vegetation as discrete land-cover types has disadvantages; however, it hides spatial and temporal variations in internal composition and structure (Williams et al., *in preparation*), replaces vegetational gradients with unrealistically abrupt boundaries, and the proliferation of various classification schemes hinders intercomparisons difficult among simulated and observed vegetation maps (DeFries et al., 1999).

Mapping plant life-form densities represents an alternative to biome-based mapping. Recently, DeFries et al. (1999, 2000) used observations from the Advanced Very High Resolution Radiometer (AVHRR) to estimate, for the globe, the percent canopy cover for plant life-forms, including needleleaved evergreen trees, broadleaved deciduous trees, and herbs. Simultaneously, coupled atmosphere–vegetation and dynamic global vegetation models are being developed (Ganopolski et al., 1998a,b; Kucharik et al., 2000) which can simulate the transient responses of vegetation to climate change. These models also rely upon plant functional types rather than biomes as the fundamental unit of vegetation. The logical next step is to reconstruct, from paleoecological data, the past distribution of plant functional types, to understand better the past interactions between climate change and land-cover change and to provide a new tool for evaluating the predictions of global vegetation models.

Fossil-pollen data provide a way to 'extrapolate' remotely sensed vegetation indices to time periods prior to the narrow window of direct observation (Williams and Jackson, *submitted for publication*). This paper presents reconstructed needleleaved and broadleaved tree-cover densities in North America since the last glacial maximum, 21,000 years before present (21 ka). In contrast to traditional mappings of fossil-pollen records (e.g. Webb et al., 1993), which assume an implicit relationship between pollen abundance and plant population density, this paper explicitly estimates past tree cover densities. The maps were obtained by finding analogs for fossil-pollen spectra in a modern-pollen dataset (Gajewski et al., 2000; Williams, 2000) and assigning to the fossil samples the AVHRR-derived tree-cover densities (DeFries et al., 1999, 2000) associated with the modern sample

sites. The analog technique used is a new variant of the modern analog technique, called the hierarchical analog technique, which enables analogs to be identified even for fossil-pollen samples that are compositionally unlike modern assemblages. The hierarchical analog technique uses the concept of plant functional types (Smith et al., 1997) to reclassify fossil-pollen spectra into functional groupings (Prentice et al., 1996), allowing the identification of functional analogs. Two levels of functional types are used. In the first level, plant taxa are grouped by life form, leaf shape, phenology, and climatic tolerance (hereafter referred to as plant functional types or PFTs). In the second level, plant taxa are grouped solely according to life form, leaf shape, and phenology (hereafter referred to as plant life-forms). The analog technique is successively repeated for pollen types, PFTs, and plant life-forms until compositional or functional analogs are identified for all fossil-pollen assemblages.

I first test the ability of the technique to reproduce present-day distributions of needleleaved and broadleaved tree-cover, then apply the hierarchical analog technique to a dataset of North American fossil-pollen records to describe changes in tree-cover since the last glacial maximum. The combination of fossil-pollen data and satellite-based observations is a powerful one, enabling the extrapolation of satellite-derived vegetation datasets beyond the limited domain of direct observation, and making it possible to study the patterns and impacts of land-cover change at millennial timescales.

2. The modern and hierarchical analog techniques

2.1. Modern analog technique—overview

The modern analog technique (MAT) is widely employed to infer past environments from micropaleontological assemblages such as pollen (Guiot, 1990; Bartlein and Whitlock, 1993; Cheddadi et al., 1998; Jackson et al., 2000; Williams et al., 2000a) and marine diatoms and foraminifera (Prell, 1985; Thunell et al., 1994; Pflaumann et al., 1996; Crosta et al., 1998; Waelbroeck et al., 1998). The central assumption of the modern analog technique is based upon reasoning by analogy: if two paleontological assemblages contain a similar mixture of fossils, then the communities that produced these assemblages must also have been similar (Overpeck et al., 1985). By further assuming that community composition is determined by and in dynamic equilibrium with external environmental factors, such as climate (Webb, 1986; Prentice et al., 1991), the modern analog technique can be applied to infer past environmental conditions from paleoecological assemblages. Application of the MAT requires a dataset of microfossil assemblages from coretops and other modern sediments, for which local ecosystem and environmental properties are known. Fossil assemblages are matched to modern assemblages and assigned the properties of their modern analogs.

A variety of measures exists to measure the multivariate distance between pollen assemblages, with the squared chord distance most commonly used (Overpeck et al., 1985; Prell, 1985). Methods for the selection of analogs vary among studies. Often, an empirically derived threshold distance discriminates between matching vs. non-matching samples (Overpeck et al., 1985). Alternatively, a fixed number of best analogs can be retained (usually 10). Neither approach is ideal, because dissimilarity values are affected by the species richness and evenness of the sampled community, and the number of analogs for a fossil sample may vary widely (Waelbroeck et al., 1998). The range of analogs can be constrained by independent sources of information, such as lake levels (Guiot et al., 1993; Cheddadi et al., 1997) or geographic distance (Pflaumann et al., 1996; Williams et al., 2000a). The standard deviation of each analog-based estimate can be calculated from the range of values associated with the modern analogs for an individual sample.

A major limitation of the modern analog technique is that it cannot make a meaningful assignment for a fossil-pollen sample with no good analog in the modern dataset. Changes in the realized environmental space (Jackson and Overpeck, 2000) during the Quaternary have resulted in past plant associations with no modern counterpart. In North America and Europe, plant associations unlike any today were widespread between 17 and 12 ka (Anderson et al., 1989; Huntley, 1990; Overpeck et al., 1992; Williams et al., 2001). The classical form of the analog technique (Overpeck et al., 1985) is useful for identifying

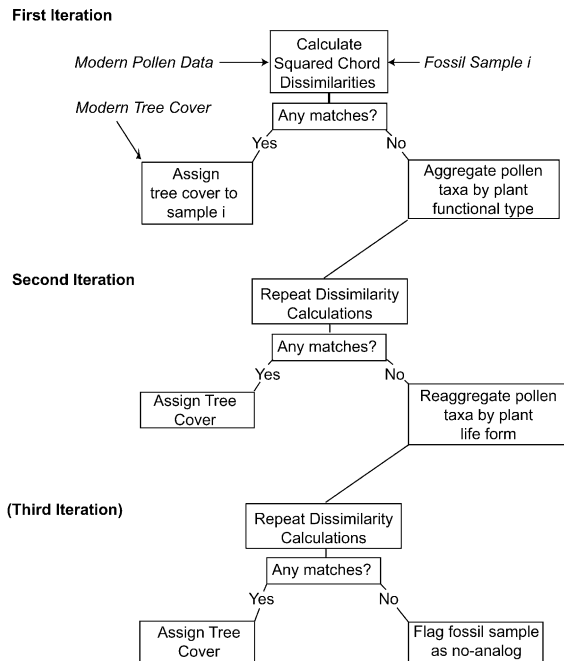


Fig. 1. Flowchart outlining the key steps of the hierarchical analog technique. In the first level of analog-matching, the squared chord distances (SCDs) between a fossil-pollen sample i and modern-pollen samples are measured, using the percent abundance of individual pollen taxa as the unit of comparison (Overpeck et al., 1985). The tree-cover estimates associated with the ‘best’ modern analogs (criteria described in Section 2) are averaged and assigned to the fossil-pollen sample. If no good modern analogs exist, the fossil-pollen sample is subjected to a second iteration of the modern analog technique. In the second level of analysis, the pollen taxa in the modern- and fossil-pollen samples are reaggregated to plant functional types, and dissimilarities recalculated. In an experimental third level of analysis, the fossil- and modern-pollen samples were reclassified into simple life forms, but the high uncertainties associated with this level analysis meant that only the assignments made by the first two analyses were included in the paleovegetation reconstructions.

periods of dissimilar vegetation and environments but alone cannot further constrain their environmental properties (Williams et al., 2001).

2.2. Hierarchical analog technique

This study presents a new variant of the modern analog technique, called the hierarchical analog technique (HAT), which provides a formalized method for generalizing pollen data according to functional sim-

ilarities, so that analogs can be found even when a fossil-pollen sample has no compositional analog in the modern-pollen data (Fig. 1). The first level of the hierarchical analog technique is identical to the standard modern analog technique (Fig. 1): the squared chord distances (SCDs) among modern- and fossil-pollen samples are calculated, using individual pollen taxa as the units of comparison, and fossil-pollen samples with modern analogs are assigned the environmental properties associated with the modern samples. A low SCD indicates a close similarity between two pollen samples. The ‘jump’ method (Waelbroeck et al., 1998) determines which modern assemblages are sufficiently similar to the fossil sample to be considered analogs: the modern assemblages are sorted by their squared chord distance from the fossil-pollen sample, and large differences (jumps)

Table 1

List of plant functional types, life forms, and abbreviations

Category	Abbreviation
<i>Plant functional types</i>	
Boreal Evergreen Conifer/ Cool Temperate Conifer	BEC/CTC
Boreal Summergreen Conifer	BSC
Cool Temperate Conifer	CTC
Warm Temperate Conifer	WTC
Eurythermic Conifer	EC
Boreal Summergreen/ Cool Temperate Summergreen	BS/TS1
Temperate Summergreen	TS
Cool Temperate Summergreen	TS1
Warm Temperate Summergreen	TS3
Temperate Summergreen/ Warm Temperate Evergreen	TS/WTE
Warm Temperate Evergreen/ Schlerophyll Shrub	WTE/SS
Broadleaved Shrub	BSH
Forb	Forb
Sedge	Sedge
Grass	Grass
Heath	Heath
<i>Plant life forms</i>	
Deciduous Broadleaf	DB
Deciduous Needleleaf	DN
Evergreen Broadleaf	EB
Evergreen Needleleaf	EN
Herb/Small Shrub	Herb
Graminoid	Gram

Table 2
Assignment of pollen taxa to plant functional types

	Functional types	Life forms
<i>Abies</i>	BEC/CTC	EN
<i>Acer</i>	TS	DB
<i>Alnus</i> undif.	TS1, BSH ^a	DB
<i>Ambrosia</i> -type	Forb	Herb
Apiaceae	Forb	Herb
Aquifoliaceae	WTE/SS	EB
<i>Artemisia</i>	Forb	Herb
Asteraceae/Tubuliflorae	Forb	Herb
<i>Betula</i> undif.	BS/TS1, BSH ^a	DB
Brassicaceae	Forb	Herb
<i>Carya</i>	TS	DB
Caryophyllaceae	Forb	Herb
<i>Castanea</i>	TS	DB
<i>Ceanothus</i>	TS/WTE	DB
<i>Celtis</i>	TS	DB
<i>Cephalanthus</i>	BSH	DB
<i>Cercocarpus</i>	WTE/SS	EB
Chenopodiaceae/Amaranthaceae	Forb	Herb
<i>Clethra</i>	BSH	DB
<i>Corylus</i>	BSH	DB
Cupressaceae/Taxaceae	EC	EN
Cyperaceae	Sedge	Gram
<i>Dryas</i>	Forb	Herb
<i>Ephedra</i>	Forb	Herb
Ericaceae	Heath	EB
<i>Eriogonum</i>	Forb	Herb
Euphorbiaceae	Forb	Herb
<i>Fagus</i>	TS1	DB
<i>Fraxinus</i>	TS	DB
<i>Juglans</i>	TS	DB
<i>Larix/Pseudotsuga</i>	BSC	DN
<i>Liquidambar</i>	TS3	DB
Myricaceae	BSH	EB
<i>Nyssa</i>	TS3	DB
<i>Ostrya/Carpinus</i>	TS	DB
<i>Oxyria</i>	Forb	Herb
<i>Picea glauca</i>	BEC/CTC	EN
<i>Picea mariana</i>	BEC/CTC	EN
<i>Picea</i> undif.	BEC/CTC	EN
<i>Pinus strobus</i>	CTC	EN
<i>Pinus</i> undif.	EC	EN
<i>Platanus</i>	TS	DB
Poaceae	Grass	Gram
<i>Populus</i>	BS/TS1	DB
<i>Quercus</i>	TS, TS/WTE ^b	DB
Ranunculaceae	Forb	Herb
Rubiaceae	WTE/SS	EB
<i>Salix</i>	TS1, BSH ^a	DB
<i>Sarcobatus</i>	Forb	Herb
Saxifragaceae	Forb	Herb
<i>Shepherdia</i>	BSH	DB
<i>Taxodium</i>	WTC	EN
<i>Tilia</i>	TS1	DB

Table 2 (continued)

	Functional types	Life forms
<i>Tsuga</i>	CTC	EN
<i>Ulmus</i>	TS	DB

^a *Alnus*, *Betula*, and *Salix* are classified as broadleaved shrub if the pollen sample was assigned to tundra, mixed parkland, or spruce parkland biomes.

^b *Quercus* was assigned to the mixed-plant functional type temperate-summergreen/warm-temperate-evergreen if the pollen sample was assigned to warm mixed forest or xerophytic woods/scrub.

in the ordered list of distances are identified. A jump is defined to occur when a SCD is at least 1.2 times greater than the previous distance. This jump threshold is chosen empirically, and the analog results are insensitive to threshold values between 1.1 and 1.3 (Waelbroeck et al., 1998; Williams, unpublished data). Only those modern samples with SCDs less than the jump point are retained as analogs. If no jumps occur before a SCD of 0.15 is reached, all analogs with distances <0.15 are retained. The needleleaved and broadleaved tree-cover estimates associated with the modern analogs (see below) are averaged and assigned to the fossil-pollen sample. If all SCDs are greater than 0.15, the fossil-pollen sample is set aside for the second level of the hierarchical analog technique.

In the second level, the modern- and fossil-pollen data are regrouped into 16 plant functional types (Tables 1 and 2), defined according to life form, phenology, leaf shape, and climatic tolerance (Prentice et al., 1996). Certain pollen types can be assigned to more than one plant functional type (Prentice et al., 1996), because either several species representing different PFTs cannot be distinguished palynologically (e.g. the *Populus* pollen type includes *Populus balsamifera*, a boreal summergreen, and *P. deltoides*, a temperate summergreen), or because the functional characteristics of a single species are plastic (e.g. phenology may vary according to local moisture availability and growing season length). For these taxa, I created several mixed-PFT categories (Table 1). In a few ambiguous cases (Table 2), the PFT assignment is determined by the biome assignment for the sample (Peyron et al., 1998, 2000). After the pollen taxa in the modern and remaining fossil-pollen samples are reaggregated to PFTs, squared-chord distances are recalculated, analogs identified using the

same algorithms and rules defined above, and the remaining fossil-pollen samples with no close matches set aside for the third analysis.

In the third and final analysis, the pollen taxa are reclassified into six plant life-form categories (Tables 1 and 2) based solely upon life form, phenology, and leaf shape. Squared-chord distances are recalculated and analogs assigned, again using the rules defined above. All remaining fossil-pollen samples were assigned an analog in the third level of resolution. Thus, with each level of analysis, the resolution of the pollen data coarsens, but in a manner consistent with the goal of assigning vegetation type. In Section 4, I evaluate the ability of each level of analog analysis to reproduce present-day distributions of needleleaved and broadleaved tree-cover.

For the paleovegetational reconstructions, modern-pollen samples were omitted from the analysis if they were collected from regions heavily altered by human activity. I determined the land-cover type for each pollen sample from the DISCover land-cover dataset (Loveland et al., 2000) by placing a 20×20 km window around each pollen site and retaining the modal land-cover type. Modern-pollen samples from regions classified as Croplands, Urban and Built-Up, and Cropland/Natural Vegetation Mosaic were not used.

3. Data

3.1. Pollen data

The modern-pollen dataset consists of 4571 surface pollen samples (Fig. 3), drawn from the Global Pollen Database (<http://www.ngdc.noaa.gov/paleo/gpd.html>), a dataset of surface pollen samples from the western US (Davis, 1995), and data holdings at Brown University (Avizinin and Webb, 1985; Williams, 2000) and the University of Ottawa (Gajewski et al., 2000). The raw counts for 55 pollen types (Table 2) were extracted from the modern-pollen dataset and converted to percent form, using the same taxa for the pollen sum. The fossil-pollen dataset consists of 759 cores, drawn mainly from the North American Pollen Database (<http://www.ngdc.noaa.gov/paleo/napd.html>), and supplemented with mid-Holocene data from the PALE Beringian Working Group

(1999), and the Base de Données Polliniques et Macro-fossiles du Québec (P. Richard, personal communication; Williams, 2000). Site density in this dataset is good for eastern and boreal North America, but poor for the western US.

For display purposes, pollen percentages were interpolated to a 50-km grid, using an Albers equal-area projection (Snyder, 1982) with standard parallels at 66.67°N and 33.33°N and the origin set to 50°N , 120°W . Pollen percentages were interpolated from individual site locations to the grid points using a distance-weighted tri-cubic spline (Williams et al., 2001). The pollen percentages are mapped in isopoll form, with contours of equal pollen abundance (Bernabo and Webb, 1977). A pollen site was included if it was within a search window centered on a gridpoint, with half-width dimensions of $750 \text{ km} \times 750 \text{ km}$ (horizontal) $\times 500 \text{ m}$ (vertical). Including the vertical dimension in the distance weighting accommodates the effect of elevation upon vegetation composition and pollen assemblages. Coastline and ice-sheet positions for the past 21,000 years are from Bartlein et al. (1998).

3.2. AVHRR-inferred maps of tree-cover

The present-day estimates of needleleaved and broadleaved tree-cover were produced by DeFries et al. (1999) from AVHRR observations between 1992 and 1993. They generated thirty metrics from the AVHRR data to characterize the annual cycle of leaf growth and senescence, and defined three end-member states: woody vegetation, herbaceous vegetation, and bare ground. A linear mixing model was applied to estimate, for each pixel, the proportion covered by each end-member. In North America, the woody vegetation was split into needleleaved evergreen trees and broadleaved deciduous trees based on seasonal variations in AVHRR observations. This classification works well for most of the vegetation in North America, except for vegetation types with significant proportions of broadleaved tree taxa (e.g. subtropical forest, chaparral). Again, a linear mixing model was used to discriminate between these two types. Low-lying shrubs tended to be classified as herbaceous cover. Woody coverages less than 10% were set to 0% and coverages greater than 80% were set to 80% (DeFries et al., 1999). Total tree cover is defined as

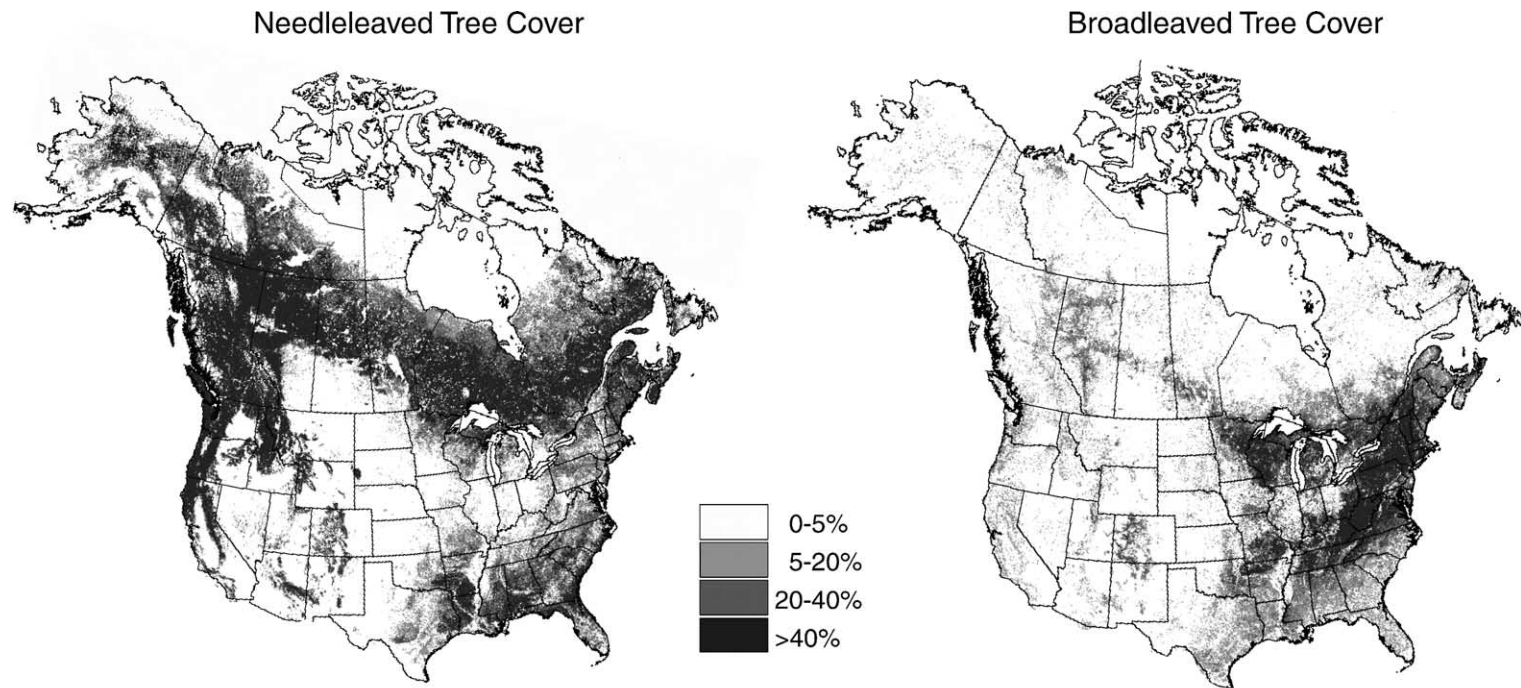


Fig. 2. Broadleaved and needleleaved percent tree-cover in North America, as inferred from AVHRR observations collected between 1992 and 1993. Redrawn from DeFries et al. (1999).

the sum of the needleleaved and broadleaved tree coverages for each grid point. Bare ground and herbaceous cover occupies the fraction of each pixel not covered by tree canopy.

The resultant tree-cover maps (Fig. 2) indicate well-defined zones of needleleaved and broadleaved trees in North America that are consistent with other land-cover reconstructions (DeFries et al., 1999). Needleleaved tree-cover densities are highest in the boreal forests, dominated by *Abies*, *Picea*, and *Pinus*, and in the montane forests and woodlands of the western US, where *Abies*, *Larix*, *Juniperus*, *Picea*, *Pinus*, *Pseudotsuga*, *Thuja*, and *Tsuga* dominate (Küchler, 1964; Rowe, 1972; Elliott-Fisk, 2000; Peet, 2000). Needleleaved tree-cover densities are moderate in the southeastern US, where stands of *Pinus* mix with *Quercus*, *Carya*, *Magnolia*, *Nyssa*, *Liquidambar*, *Fraxinus*, *Acer*, and other angiosperms (Braun, 1950; Christensen, 2000). High broadleaved tree-cover densities are confined to the deciduous forests of the eastern United States. Key taxa include *Acer*, *Betula*, *Carya*, *Fagus*, *Fraxinus*, *Liriodendron*, *Quercus*, *Tilia*, and *Ulmus*. Tree densities are low in the semi-arid western US, in Arctic Canada and Alaska, and in areas converted to agriculture.

3.3. Assigning AVHRR values to modern-pollen sites

The pollen source-area for lakes depends upon the size of the lake basin and the species-specific dispersal properties of the pollen grains (Prentice, 1988). The pollen and AVHRR estimates of needleleaved and broadleaved abundance are best correlated for search-window half-widths between 25 and 100 km (Williams and Jackson, submitted for publication). This spatial scale is consistent with other empirical studies of pollen source-area (Bradshaw and Webb, 1985; Prentice et al., 1987; Jackson, 1990, 1991) and physical models of pollen dispersal (Prentice, 1985, 1988; Sugita, 1994; Sugita et al., 1999). For this paper, a square search-window with a half-width of 75 km was centered on each modern-pollen site, and the AVHRR estimates of needleleaved and broadleaved tree density from all pixels within the window were averaged. AVHRR pixels over water bodies >1 km² were removed by application of a water mask derived from the DISCover land-cover map (Loveland et al., 2000).

4. Results

4.1. Isopoll maps

The isopoll maps for individual plant taxa (Fig. 3) correspond closely to the DeFries et al. (1999) maps of needleleaved and broadleaved tree density (Fig. 2). In general, the distribution of each pollen type occupies a subset of the area occupied by its life form. High pollen abundances for *Picea*, *Pinus*, and *Abies* are concentrated in the northern belt of needleleaved trees. Pollen samples from the needleleaved montane/subalpine forests in western North America have high abundances of *Pinus*, *Abies*, *Larix/Pseudotsuga*, and *Tsuga*. Cupressaceae pollen abundances are highest in the western US, due primarily to the influx of *Juniperus* pollen from small trees and shrubs growing in open conifer woodlands and shrublands (Küchler, 1964). *Tsuga* pollen abundances are also high in the northeastern US, in the transitional zone between needleleaved- and broadleaved-dominated forests. *Pinus* predominates in pollen samples collected from the southeastern mixed forests.

The isopoll maps for broadleaved tree taxa comprise three categories. First, for many temperate deciduous taxa the region of high pollen percentages spans the region of high broadleaved tree densities in the eastern US (e.g. *Quercus*, *Carya*, and *Ulmus*), consistent with the widespread presence of these taxa in the eastern deciduous forests (Braun, 1950). Second, the pollen abundances for taxa such as *Alnus*, *Betula*, and *Salix* have bimodal distributions, with the highest percentages north of treeline, and secondary maxima in the south. For all three taxa, the bimodal pollen distributions correspond to differing population centers for tree and shrub varieties (e.g. *Alnus crispa*, *Betula nana*, *Salix arctica* north of treeline and *A. rubra*, *B. papyrifera*, *B. lenta*, *S. nigra* in the south). The tree-cover classification algorithm used for the AVHRR data tends to be insensitive to the presence of woody shrubs (DeFries et al., 1999). Finally, some broadleaved taxa have restricted pollen distributions relative to the distribution of broadleaved trees. High abundances of *Populus* occur in a narrow band along the prairie-forest ecotone in Alberta, Saskatchewan, and Manitoba, and in the northern Canadian Rockies. High *Fagus* and *Acer* pollen abundances are closely associated with *Tsuga* in the northeastern US mixed

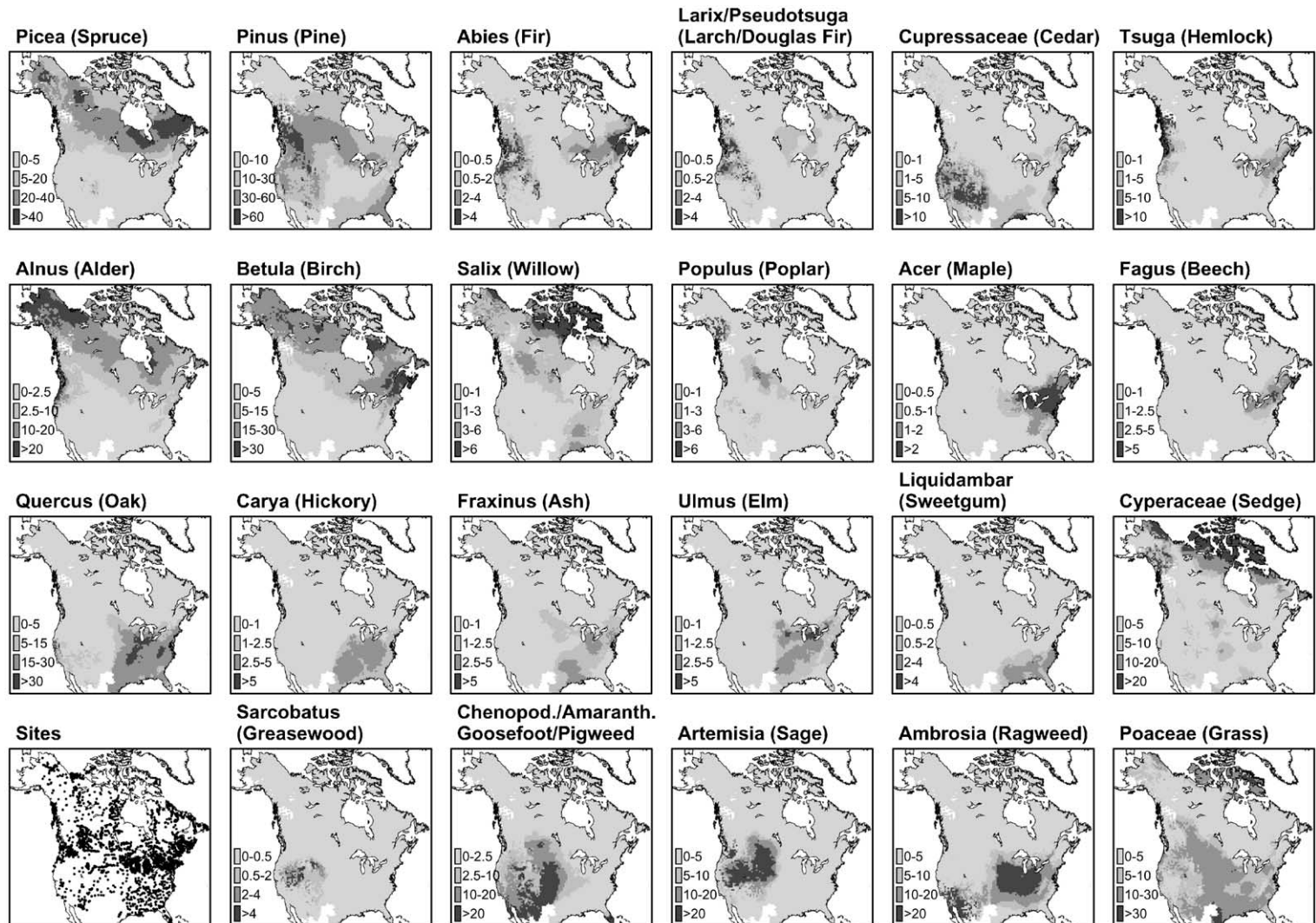


Fig. 3. Isopoll maps showing percent pollen abundances for various plant taxa, interpolated from surface sediment samples collected across North America. Darker grays correspond to higher percentages, and areas with no available pollen samples are white. The contour intervals used for each map are indicated in its lower left corner. The lower-left map shows the location of the surface samples used to construct the isopoll maps.

forests. Pollen samples containing *Liquidambar* are confined to the southeastern mixed forest. The pollen-percentage distributions for these taxa are consistent with population densities for the corresponding tree taxa (Delcourt et al., 1984).

Pollen percentages for herbaceous and shrub types (Cyperaceae, Poaceae, Chenopodiaceae/Amaranthaceae, *Sarcobatus*, *Artemisia*, and *Ambrosia*) are highest in areas of low tree density. Cyperaceae pollen abundances are highest in samples collected north of treeline, whereas *Artemisia* and *Sarcobatus* are most abundant in the arid basins of the western US and the western plains. Chenopodiaceae/Amaranthaceae pollen is most abundant in the Great Plains and in the southern deserts. Poaceae pollen is abundant in the Midwestern plains and in the southeastern US. *Ambrosia* is common in the southwestern deserts and in regions converted to agricultural use.

Overall, the patterns expressed in the isopoll maps and the maps of needleleaved and broadleaved tree-cover are similar. However, no single pollen taxon spans the range of its corresponding tree-cover type. The needleleaved and broadleaved tree-cover distributions thus provide a taxonomically coarse but spatially resolved description of the vegetation in North America that encompasses the ranges of individual species and genera. These regional variations in vegetation composition challenge the ability to define a continental-scale transfer function between the pollen-percentage data and tree-cover densities; such functions work best when applied at regional scales (Bartlein et al., 1984; Huntley and Prentice, 1988). A key advantage of the modern analog technique is that no such function is required.

4.2. Testing the hierarchical analog technique

The ability of the hierarchical analog technique to reproduce vegetation physiognomy can be tested with the modern data by running the HAT for each modern-pollen sample, and comparing its estimates of needleleaved and broadleaved tree-cover to the actual values for the modern sample locations (Fig. 4). The modern-pollen sample is not allowed to match to itself, nor to any other modern sample within 50 km. This geographic constraint minimizes the effects of spatial autocorrelation caused by overlapping pollen source-areas among nearby surface samples. For this test

only, each level of analog analysis included all modern-pollen samples, rather than only the unmatched samples from the previous level of analysis. This provides a fairer test of the accuracy of each level of analysis.

The agreement between the estimated and observed tree-cover densities is very good ($r_{\text{broad}}=0.93$, $r_{\text{need}}=0.81$) when all pollen taxa are used (Fig. 4, top). When the pollen taxa are grouped into 16 functional groups, the correlation remains strong but slightly reduced ($r_{\text{broad}}=0.89$, $r_{\text{need}}=0.76$). When the pollen taxa are grouped into six life forms, there is only a moderate to weak correlation between the estimated and observed tree densities ($r_{\text{broad}}=0.60$, $r_{\text{need}}=0.49$). For all analyses, the correlation between the estimated and observed values is stronger for the broadleaved trees than for the needleleaved trees. The slope of the best-fit regression line is close to one for all analyses, suggesting minimal systematic bias in the analog estimates.

The precision of each individual estimate can be inferred from the standard deviation of the tree-cover values associated with the modern analogs (Bartlein and Whitlock, 1993). Fig. 5 shows the distribution of standard deviations for each level of analysis. The uncertainties are smallest for the compositional analogs (median_{broad}=2.4%, median_{needle}=7.0%), intermediate for plant functional types (median_{broad}=3.5%, median_{needle}=7.8%), and when pollen taxa are regrouped into life forms (median_{broad}=5.9%, median_{needle}=9.1%).

The above tests show that the HAT accurately estimates present-day needleleaved and broadleaved tree-cover, for the first two levels of analysis. However, the power of the analog technique declines as the pollen data are aggregated into fewer categories, and by the third level, the correlation between the predicted and observed tree cover densities appears to be too low to be useful for paleoenvironmental reconstruction. Thus, when mapping the analog estimates (Figs. 6 and 7), only the results from the first two levels are included, and the functional analogs (level 2) are used only if no compositional analogs are available for a pollen sample (Fig. 1). Pollen samples with no compositional or functional modern-analogs are not included in the tree-cover reconstructions.

Maps of the present-day needleleaved and broadleaved tree-cover visually confirm a very good agree-

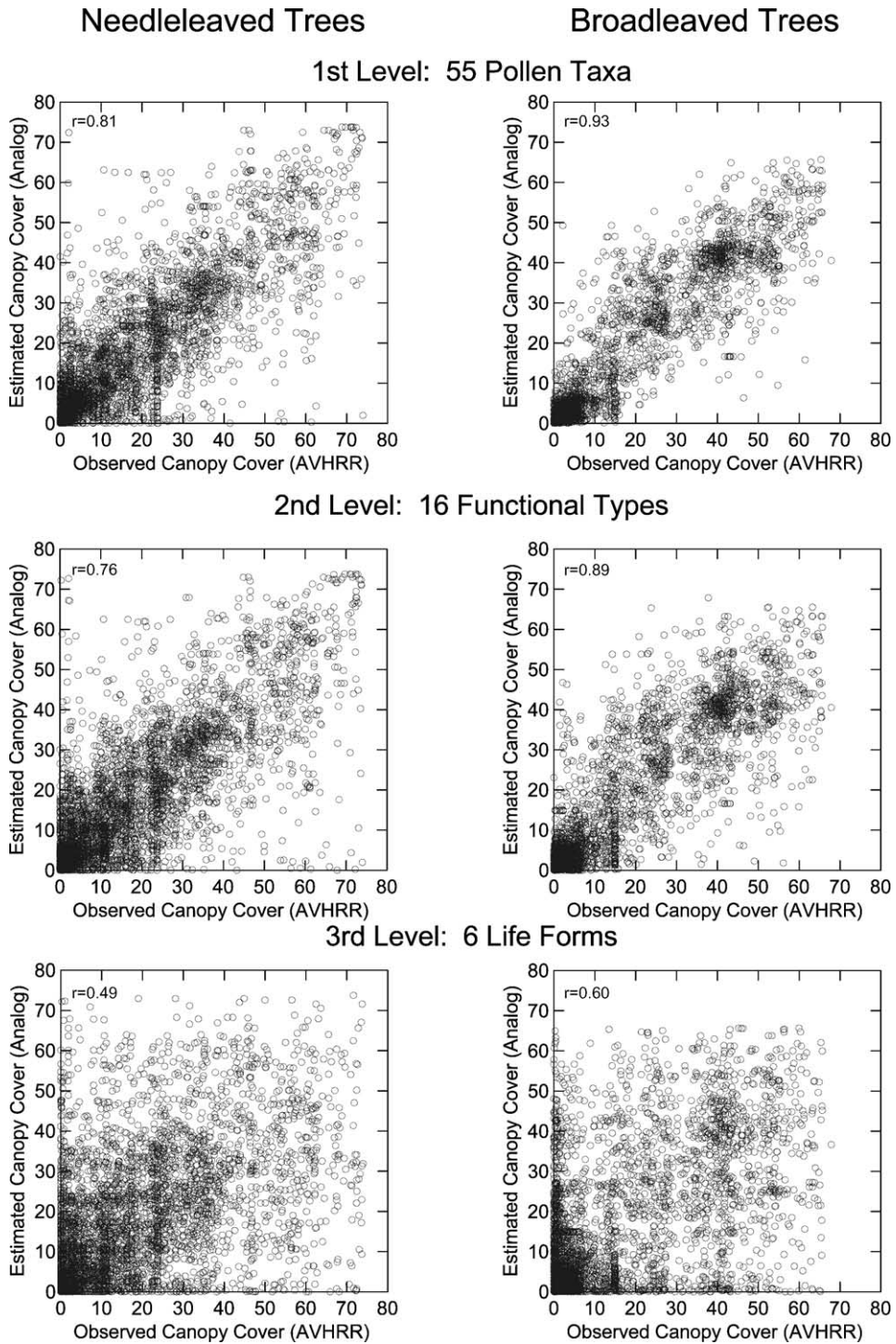
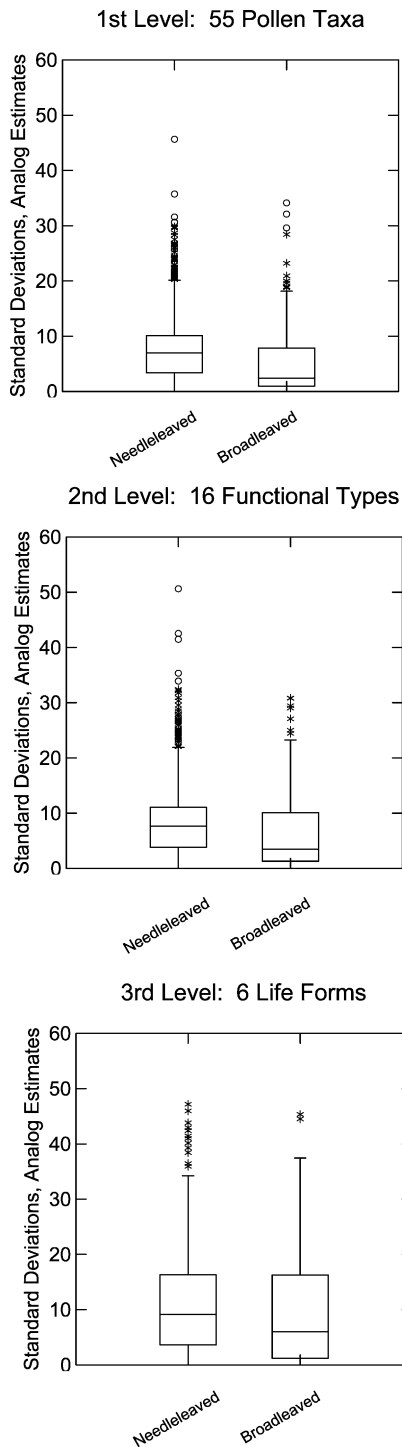


Fig. 4. Scatter plots comparing the needleleaved and broadleaved percent tree-cover observed at the surface pollen sites to the values estimated by the analog technique. The results for each level of the hierarchical analog technique are presented separately.



ment between the estimated and observed patterns of needleleaved and broadleaved tree-cover in North America (Fig. 6). Differences between the reconstructed maps of tree density and the original AVHRR-derived maps (Fig. 2) are due to (1) errors in the analog reconstructions and (2) artifacts of the spatial interpolation and the variable density of the modern-pollen network. A loss of resolution is unavoidable due to the low density of pollen sample locations relative to the 1 km AVHRR grid. To isolate the effects of the analog method, the interpolated values for the analog estimates (Fig. 6, bottom) and the original needleleaved and broadleaved tree densities assigned to the modern-pollen dataset (Fig. 6, top) were mapped. The analog estimates show a slightly smaller range of variation than the original observations, but in general the two sets of maps agree well in both pattern and magnitude. Localized discrepancies occur in Alaska, where the analog reconstructions underestimate broadleaved tree cover densities, and in the central US, where the analog reconstructions overestimate tree density. The Alaskan discrepancy is due to limitations of the surface sample dataset used, which is relatively sparse in Alaska (Fig. 3), reducing the number of possible close analogs. The discrepancy in the central US is due to the identification of analogs from regions of the deciduous forest less affected by human land-use.

4.3. Variations in tree cover since the last glacial maximum

At the last glacial maximum (21 ka), tree densities were low to moderate in eastern North America and treeless conditions prevailed in Beringia and the Pacific Northwest (Fig. 7, row 1). Between 21 and 14 ka, tree-cover densities increased in the Pacific Northwest and southeastern US, and declined in the upper Midwest. Between 14 and 11 ka, tree densities increased rapidly throughout the eastern US, and a strong east–west gradient developed between the eastern forests and interior grasslands. The forest–

Fig. 5. Box plots showing the distribution of the standard deviations associated with the individual estimates of percent needleleaved and broadleaved tree-cover, for each level of the hierarchical analog technique. The boxes mark the 25th, median, and 75th percentiles; the length of each whisker is 1.5 times the interquartile range. The median standard deviation increases with successive levels of analysis.

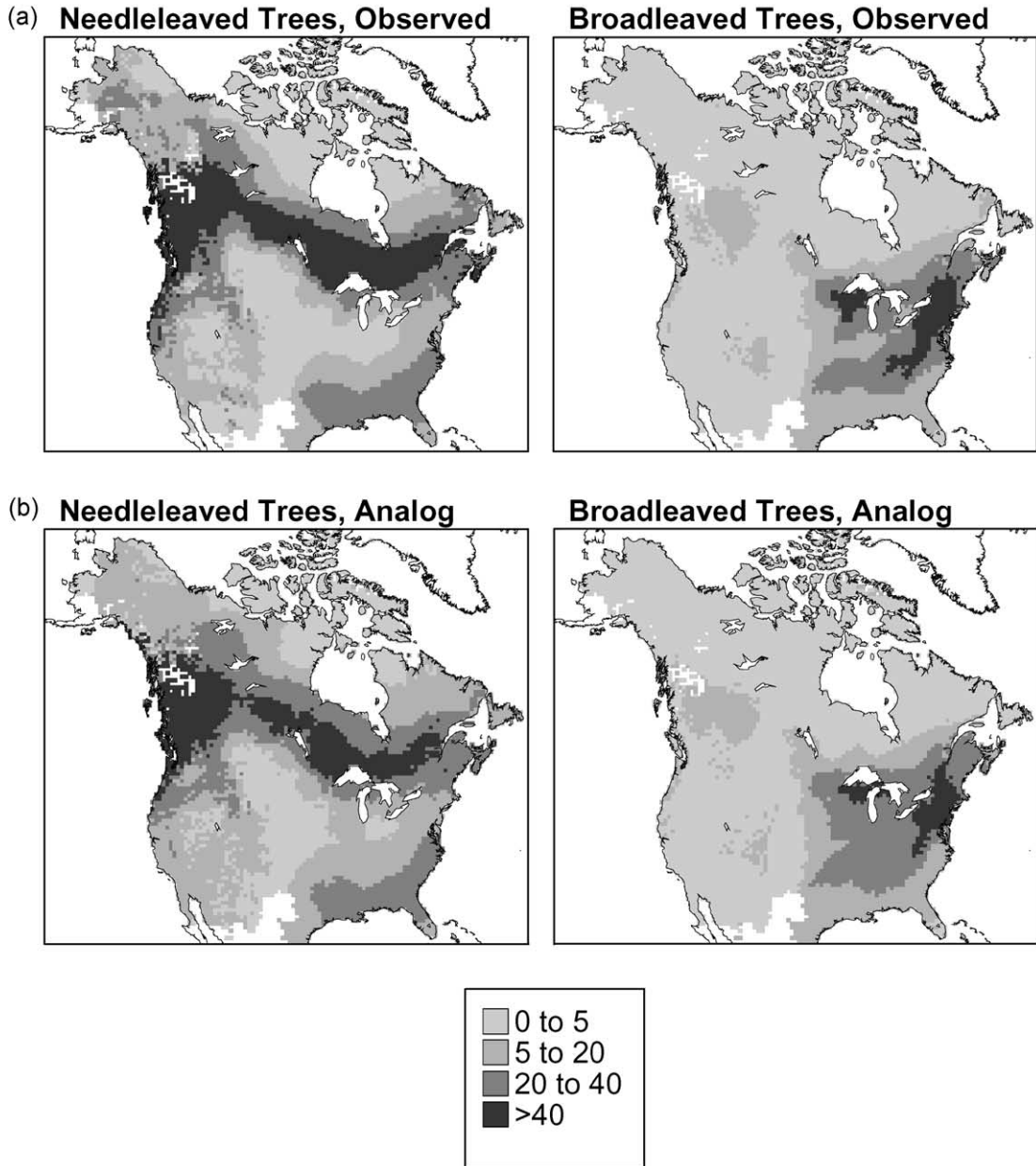
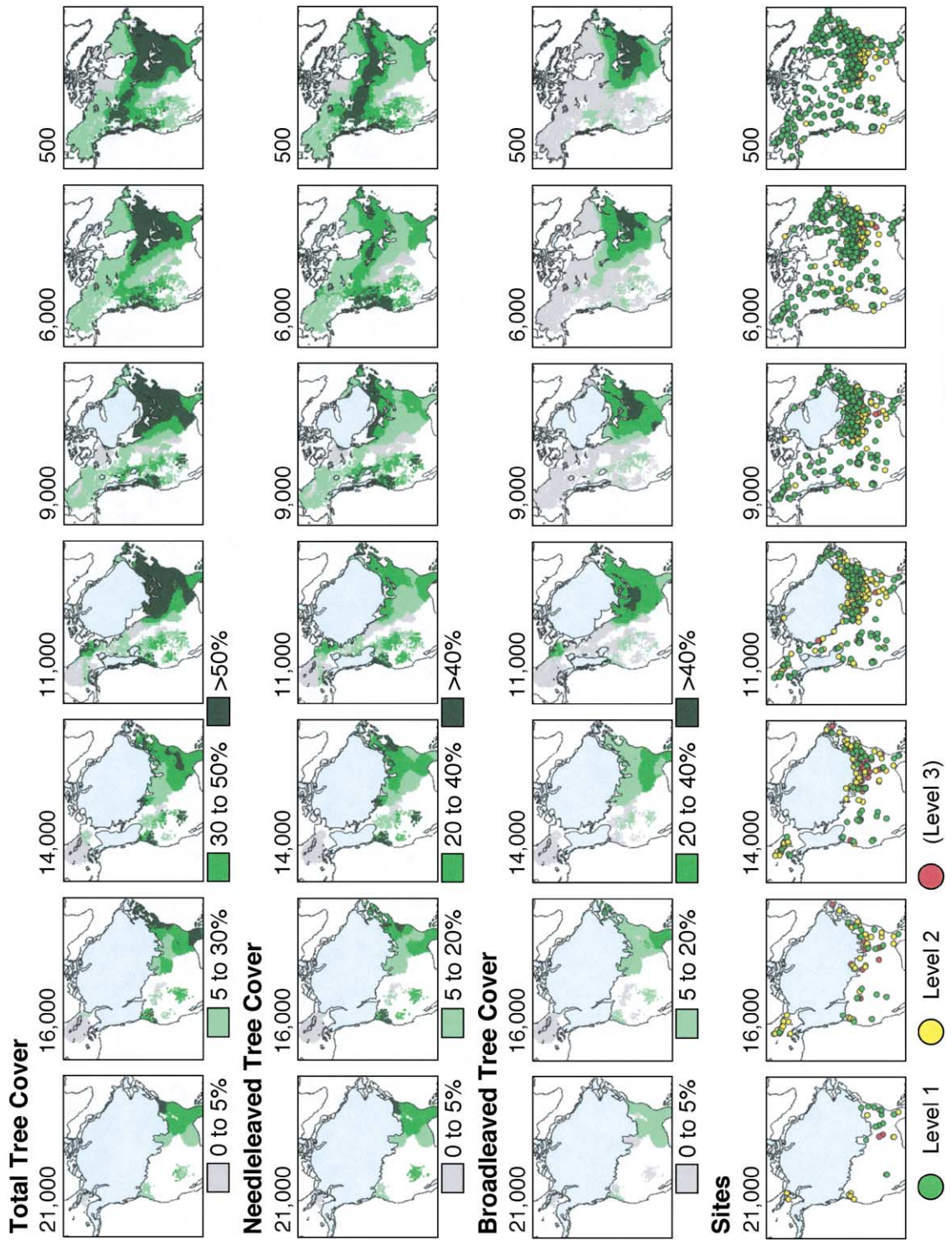


Fig. 6. Maps of present-day tree-cover, spatially interpolated from the values assigned to individual pollen sites. (a) Percent tree-cover for needleleaved and broadleaved trees, interpolated from the AVHRR-derived values assigned to each surface sample location. Differences between (a) and Fig. 2 are due to the variable density of the pollen sample network and the smoothing produced by the spatial algorithm. (b) Percent tree-cover, as estimated using the hierarchical analog technique, levels 1 and 2. The two sets of maps closely agree.

grassland transition shifted eastward during the early Holocene, then westward after 6 ka (Webb et al., 1983). In northwestern North America, low tree

densities persisted several thousand years after deglaciation, contrasting with the rapid colonization of deglaciated regions in eastern North America. Tree



cover increased in western North America during the early Holocene and by 6 ka the western and eastern boreal forests had joined. Tree density increased slowly during the late Holocene.

Needleleaved taxa dominated full-glacial forests, but needleleaved densities were lower than in the modern boreal forest (Fig. 7, row 2). Between 21 and 11 ka, needleleaved trees in the eastern US split into northern and southern groups, as cold-tolerant conifers (e.g. *Picea*, *Pinus*, and *Abies*) migrated northward (Webb et al., 1993) and broadleaved tree densities increased in the eastern US. Three zones of needleleaved forests had developed by 14 ka: a belt of conifers along the southern margin of the Laurentide Ice Sheet, another in the Pacific Northwest and Rocky Mountains, and a third in the southeastern US. The northern conifers expanded northward and westward as the Laurentide Ice Sheet retreated, linking with the western conifers by 6 ka. In the early Holocene (9 ka), needleleaved tree densities apparently were highest immediately south to the Laurentide Ice Sheet and in the Pacific Northwest. During the Holocene, needleleaved tree-cover densities in the north stabilized or slowly increased, suggesting a steady in-filling of the boreal forest.

Broadleaved tree densities were very low at the last glacial maximum (Fig. 7, row 3). A north–south gradient in broadleaved tree-cover began to develop at 16 ka and was well established at 14 ka. Broadleaved tree-cover densities rapidly increased between 14 and 11 ka, developing a unimodal distribution that persisted until 0.5 ka.

In North America, the classic regions of ‘no-analog’ vegetation occurred between 17 and 12 ka in the Great Lakes region (Cushing, 1967; Overpeck et al., 1992; Williams et al., 2001) and Beringia (Anderson et al., 1989). Most of the fossil-pollen samples from these regions were assigned functional analogs in the second level of the hierarchical analog technique (Fig. 7,

bottom). In Beringia, all of the late-glacial (17–11.5 ka) pollen assemblages have valid functional modern analogs. The late-glacial Beringian assemblages are distinguished from modern-pollen samples by high abundances of *Betula* or *Salix* pollen and low abundances of *Alnus* (Anderson et al., 1989). Because these taxa have a similar functional role (Table 2), regrouping the pollen data into plant functional types negates this distinction. Many pollen samples from the Great Lakes region continue not to have any analog, suggesting that mixtures of plant functional types not seen today covered the region. In particular, the combination of high pollen abundances of boreal conifers (*Picea*, *Abies*, and *Larix*) with herbs (Cyperaceae, *Artemisia*) and temperate deciduous trees (*Fraxinus*, *Ostrya/Carpinus*) distinguish these fossil assemblages from their modern counterparts (Williams et al., 2001). Enough assemblages have functional analogs, however, to allow tree-cover assignment and mapping.

5. Discussion

5.1. Tradeoffs in the hierarchical analog technique

At the heart of the hierarchical analog technique is a tradeoff between information loss and generality. The successive regrouping of pollen taxa into broader functional categories with each level of analysis permits functional analogs to be identified even when two pollen samples differ compositionally. This generalization allows tree-cover reconstructions even for late-glacial fossil-pollen samples which have no good compositional analogs among modern-pollen samples (Anderson et al., 1989; Overpeck et al., 1992; Williams et al., 2001). The consequence, however, of regrouping the pollen taxa into functional categories is increased uncertainty (Figs. 4 and 5), due primarily to the information lost during the successive coarsening

Fig. 7. Land-cover reconstructions for North America for 21, 16, 14, 11, 9, 6, and 0.5 ka. As in Fig. 3, increasing saturations correspond to higher tree densities, and areas left blank had insufficient data for mapping. First row: total tree-cover (sum of needleleaved and broadleaved tree cover densities), expressed in percentage form. Second row: percent needleleaved tree-cover. Third row: percent broadleaved tree-cover. Fourth row: locations of the individual pollen assemblages used to create each set of maps. Green dots indicate fossil-pollen samples that have a good compositional analog in the modern-pollen dataset. Yellow dots indicate fossil-pollen assemblages with no compositional analog in the modern dataset, but with a good functional analog. Red dots were not assigned values in the first two levels of analog analysis and were not used in the land-cover reconstruction.

from individual plant taxa to plant functional types to life forms. A key source of variance within the grouped data is intertaxonomic differences in pollen representation (Williams and Jackson, submitted for publication). For example, a *Pinus* stand and *Tsuga* stand may have similar tree-cover densities but very different pollen productivities (Jackson and Kearsley, 1998). The two stands may be indistinguishable to the AVHRR sensor, but produce very different amounts of needle-leaved tree pollen. Similar disparities exist among broadleaved taxa (e.g. *Quercus/Betula* vs. *Acer/Fraxinus*).

Thus, when applying the hierarchical analog technique to reconstruct past vegetation, I optimize it by using the full complement of pollen taxa whenever good analogs exist. Only when good compositional analogs are lacking does the method resort to regrouping the pollen data to plant functional types. These PFT-based analog estimates are subject to a greater uncertainty than the estimates based upon compositional similarity, but are able to provide reasonable constraints upon tree-cover densities for periods with compositionally distinct vegetation. With the third analysis, too much information is lost, resulting in very high uncertainties (Fig. 5) and a generally poor predictive ability (Fig. 4). Thus, for the mapped reconstructions of tree-cover (Fig. 7), only the first two levels of analysis were used.

The hierarchical analog technique could easily be applied to infer past climates from fossil pollen data, as has been done for other applications of the modern analog technique (Bartlein and Whitlock, 1993; Cheddadi et al., 1997; Gajewski et al., 2000; Jackson et al., 2000; Williams et al., 2000a), because the spatial distribution of plant functional types and life forms defined here, is primarily controlled by climate (Box, 1981; Woodward, 1987) and can be used as a proxy for climate. One advantage, however, to reconstructing properties of the past vegetation, instead of climate, is that this avoids assuming a state of equilibrium between vegetation and climate and assumptions about which aspects of climate control vegetation distributions (Huntley, 1996). However, there is no technical or theoretical obstacle to applying the HAT to reconstruct past climates. In a related effort, Peyron et al. (1998, 2000) regrouped pollen data into plant functional types and used artificial neural-network methods to infer mid-Holocene climates in Africa and Europe.

Because plant functional types have broader climatic tolerances than individual plant taxa, paleoclimatic reconstructions based upon PFT's should be less precise, but the hierarchical analog technique can at least set a constraint upon fossil-pollen samples with no compositional modern analog.

5.2. Accuracy of the tree cover reconstructions

Key determinants of the accuracy of the tree-cover reconstructions are the accuracy of the original AVHRR dataset and the completeness of the modern-pollen sample dataset. Comparison of the AVHRR data to other remotely sensed land-cover datasets suggest a good agreement (69–84%) in percent total tree-cover, with the AVHRR estimates predicting somewhat higher values for sparsely wooded locations (DeFries et al., 2000). The tree-cover estimates likely underestimate the fractional land surface covered by woody vegetation in semiarid and tundra shrublands, because the classification method relies in part upon the shadow cast by taller trees (DeFries et al., 1999). The modern-pollen dataset for North America is extensive and spatially dense (Fig. 3), but certain regions (e.g. western Alaska and northwestern US) are less well-represented and fossil pollen samples drawn from similar environments may have a poorer selection of modern analogs for matching.

The accuracy of the late-Quaternary tree-cover reconstructions cannot be fully assessed in the absence of independent information about past tree densities. The reconstructions are, however, consistent with other mappings of fossil-pollen data (Webb et al., 1993; PALE Beringian Working Group, 1999; Edwards et al., 2000; Thompson and Anderson, 2000; Williams et al., 2000b). Holocene tree-cover densities in northwestern North America appear to be somewhat low given that closed forests developed by 6 ka (Ritchie, 1987). This discrepancy echoes the underestimate of present-day tree-cover by the HAT (Fig. 5) and is probably due to the bias of the AVHRR sensor against low-lying shrubs and the relatively poor spatial coverage of the modern pollen dataset in the region. The inferred high tree-cover densities in northwestern Canada at 11 ka appears to be an overestimate caused by locally high pollen abundances of *Populus* and *Betula* (Ritchie, 1984), resulting in modern analogs drawn from the central boreal forest.

5.3. Tree-cover densities at the last glacial maximum

A striking feature of the needleleaved and broadleaved tree-cover reconstructions for the past 21,000 years is the overall increase in tree densities from relatively low levels at the last glacial maximum (Fig. 7). The low to moderate tree-cover densities for the last glacial maximum are consistent with the prevalence of open conifer woodland and parklands inferred from biome-based reconstructions of the fossil-pollen data (Jackson et al., 2000; Thompson and Anderson, 2000; Williams et al., 2000b). Many full-glacial pollen samples from eastern North America contain *Pinus* pollen percentages in excess of 80% (Whitehead, 1967; Watts, 1970, 1980), but actual tree-cover densities presumably were much lower, due to the overrepresentation of *Pinus* in pollen assemblages (Delcourt et al., 1984). An ensemble of general circulation model simulations for the last glacial maximum indicate that mean annual temperatures in unglaciated regions were colder than present by 4–14°C and that precipitation levels were somewhat lower (Joussaume and Taylor, 2000). Pollen-based climatic reconstructions (Jackson et al., 2000) for eastern North America indicate that January temperatures were 18–26°C colder than present, July temperatures were 2–18°C colder than present, and precipitation levels were 20–60% lower than present. Furthermore, due to low atmospheric CO₂ concentrations (Petit et al., 1999), plants may have been operating with decreased water use efficiencies at the last glacial maximum (Cowling, 1999). The effects of a cold and dry climate and reduced CO₂ concentrations likely worked in concert to reduce tree-cover densities at the last glacial maximum (Cowling, 1999; Levis et al., 1999). In turn, sparser tree densities in mid-to-high latitudes may have increased the surface albedo, particularly during snow-covered periods of the year (Levis et al., 1999), and should have decreased surface-roughness and evapotranspiration rates.

5.4. Complementarity of pollen and remote sensing observations

This paper demonstrates how fossil-pollen and satellite-based observations can be combined to study changes in the vegetation at timescales not amenable to remote sensing alone. Fossil-pollen records can also

be considered to be a remote sensor of the vegetation (Webb, 1981; Williams and Jackson, submitted for publication), and in general fossil-pollen records and satellite-based observations have complementary properties. Satellite-based instruments have a high temporal and spatial resolution (10¹–10³ days; 10¹–10³ m, varying by instrument), but are limited to at most 20–30 years of direct observation. Fossil-pollen records have a lower resolution (approximately 10¹–10² years and 10²–10⁵ m), but provide vegetation histories spanning 10²–10⁶ years (Prentice, 1988). The relatively long timespan of fossil-pollen records thus enables satellite-derived variables to be extrapolated beyond the limited domain of direct observation (Williams and Jackson, submitted for publication). Conversely, a key goal in pollen-based reconstructions of late-Quaternary vegetation has been to bridge the gap between the raw data (relative abundances of various pollen types) and ecologically meaningful descriptions of the past vegetation. Calibrating the modern-pollen data against satellite-based indices of the modern vegetation, which are widely available, inexpensive, and spatially precise, provides one way to bridge the gap. Satellite-based measurements of the vegetation are key inputs for process-based terrestrial ecosystem models (Field et al., 1995; Hunt et al., 1996), and the short temporal extent of satellite observations has been a major limitation for applying these models to look at longer-term ecosystem dynamics (Field et al., 1995).

This paper presents results from just one of the vegetational datasets available from satellite-based sensors. Other products include categorical land-cover classifications (DeFries et al., 1998; Loveland et al., 2000), fraction of photosynthetically active radiation absorbed by the vegetation, net primary productivity, and leaf area index (Kumar and Monteith, 1981; Goward and Dye, 1987; Nemani and Running, 1995, 1996; Hunt et al., 1996; Fassnacht et al., 1997; van Leeuwen et al., 1997). The latter three properties are closely related indices of vegetation greenness, and because these properties are in part determined by vegetation composition, for which fossil-pollen data provides a proxy, it may be possible to extrapolate them into the past. The main limitation to applying the modern analog technique globally is the availability of surface pollen samples elsewhere. At present, extensive modern datasets are available for

North America, Europe (Guiot et al., 1993; Peyron et al., 1998), western Russia (Tarasov et al., 1998), and China (Yu et al., 2000), and efforts continue to gather comparable datasets for other parts of the globe (Prentice and Webb, 1998).

5.5. *Implications of tree-cover reconstructions for global change research*

The tree-cover reconstructions presented here complement biome-based reconstructions of late-Quaternary vegetation (Edwards et al., 2000; Prentice et al., 2000; Thompson and Anderson, 2000; Williams et al., 2000b). Biomes, plant functional types, and the plant life-forms mapped here all represent vegetation structure at a level appropriate to studying broad-scale vegetation–atmosphere interactions. This includes study of vegetation responses to late-Quaternary environmental change and the reciprocal effects of changing vegetation structure upon terrestrial boundary conditions and biogeophysical feedbacks to the atmosphere. Categorical maps of the vegetation (e.g. biomes) and tree-cover densities each have advantages and disadvantages. Categorical vegetation classifications provide a relatively simple way to describe vegetation properties for a limited number of vegetation types, and are widely used (Küchler, 1964; Olson et al., 1984; Bailey, 1998; DeFries et al., 1998; Matthews, 1983; Loveland et al., 2000). Many biome definitions explicitly link biome distributions to climate (Holdridge, 1967; Box, 1981; Prentice et al., 1992), providing a convenient means to predict equilibrium vegetation distributions from simulated climates (Kutzbach et al., 1998). Mapping tree-cover densities, on the other hand, provides a better representation of the continuity of most vegetational gradients in space and time, avoiding the abrupt boundaries inherent to biome classifications (DeFries et al., 1999). The tree-cover maps similarly are better at representing spatial heterogeneity within vegetation formations or biomes, patterns that are obscured by biome maps (Williams et al., *in preparation*). There is less potential for semantic confusion than for biome reconstructions (DeFries et al., 1999); many biome classification schemes exist, challenging comparison among biome reconstructions. Both types of analyses provide useful insights into late-Quaternary environments and processes.

Data-model comparisons between climate reconstructions based upon paleoecological records and physically based climate model simulations have supplied key advances in the understanding of late-Quaternary earth system dynamics (COHMAP Members, 1988; Wright et al., 1993; Webb and Kutzbach, 1998). An increasing variety of paleoenvironmental interpretations from paleoecological datasets are available for evaluating different aspects of late-Quaternary climate simulations (Kohfeld and Harrison, 2000). The tree-cover reconstructions presented here provide an additional interface between earth system models and paleoecological data. The inferred land-cover maps can be used to provide more realistic land surface inputs for climate models, or for evaluating the results of coupled vegetation-climate models (Prentice and Webb, 1998; Kohfeld and Harrison, 2000). The development of dynamic global vegetation models (DGVMs) has enabled the study of feedbacks between the vegetation and atmosphere (Foley et al., 1998; Ganopolski et al., 1998a) and the effects of such feedbacks upon past climates (Levis et al., 1999). To simulate the transient responses of vegetation to environmental change, most DGVMs use plant functional types as their basic units of vegetation. The tree-cover maps presented here thus provide a new way to evaluate the results of dynamic vegetation models against data-based reconstructions of the past vegetation, whereas model experiments can be designed to evaluate the relative importance of low CO₂, moisture balance, and temperature for maintaining the low tree densities observed for the last glacial maximum (Levis et al., 1999).

6. Conclusions

This paper presents estimates of the percent cover for needleleaved and broadleaved trees in North America since the last glacial maximum. The reconstructions reveal a long-term increase in tree-cover densities from a low at the last glacial maximum to a maximum during the late Holocene. Low tree-cover densities at the last glacial maximum were likely caused by a combination of colder-than-present temperatures, lower-than-present precipitation levels, and lower-than-present atmospheric CO₂ concentrations. In turn, low tree-cover densities of the last glacial maximum may have re-

sulted in higher surface albedos, lowered rates of evapotranspiration, and decreased surface-roughness.

This paper is the first attempt to quantitatively estimate needleleaved and broadleaved tree-cover distributions for the late Quaternary, as well as one of the first systematic approaches to combining fossil-pollen datasets with remotely sensed indices of the modern vegetation. To reconstruct past tree-cover distributions, a variant of the modern analog technique, called the hierarchical analog technique, matches fossil and modern-pollen samples according to compositional and functional similarities. The key advantage of the hierarchical analog technique is its ability to infer past tree-cover densities even if a fossil-pollen sample has no compositional analogs in the modern-pollen data. Analog assignments based upon functional matches tend to have higher uncertainties than those based upon compositional matches, due primarily to intertaxonomic differences in pollen productivity. Tests of the hierarchical analog technique show that it is capable of reproducing the present-day distributions of needleleaved and broadleaved tree-cover with a high degree of accuracy.

Acknowledgements

This work was conducted while the author was a postdoctoral associate at the National Center for Ecological Analysis and Synthesis, a Center funded by NSF (Grant #DEB-0072909), the University of California, and the Santa Barbara campus. I thank K. Gajewski, M. Sawada, and A. Viau for their assistance in developing the surface pollen dataset. The North American Pollen Database and Global Pollen Database are public resources maintained by the National Geophysical Data Center, and are the result of generous data contributions by the palynological community. Comments from S. Jackson, R. DeFries, P. Bartlein, P. Moss, and an anonymous reviewer improved this manuscript.

References

- Adams, J.M., Faure, H., 1998. A new estimate of changing carbon storage on land since the last glacial maximum, based on global land ecosystem reconstruction. *Global and Planetary Change* 16–17, 3–24.
- Anderson, P.M., Bartlein, P.J., Brubaker, L.B., Gajewski, K., Ritchie, J.C., 1989. Modern analogs of late-Quaternary pollen spectra from the western interior of North America. *Journal of Biogeography* 16, 573–596.
- Avizinis, J., Webb III, T., 1985. The Computer File of Modern Pollen and Climatic Data at Brown University. Unpublished.
- Bailey, R.G., 1998. *Ecoregions: The Ecosystem Geography of the Oceans and Continents*. Springer, New York, 176 pp.
- Bartlein, P.J., Whitlock, C., 1993. Paleoclimatic interpretation of the Elk Lake pollen record. In: Bradbury, J.P., Dean, W.E. (Eds.), *Elk Lake, Minnesota: Evidence for Rapid Climate Change in the North-Central United States*. Geological Society of America Special Paper. Geological Society of America, Boulder, CO, pp. 275–293.
- Bartlein, P.J., Webb III, T., Fleri, E., 1984. Holocene climate change in the northern Midwest: pollen-derived estimates. *Quaternary Research* 22, 361–374.
- Bartlein, P.J., Anderson, K.H., Anderson, P.M., Edwards, M.E., Mock, C.J., Thompson, R.S., Webb, R.S., Webb III, T., Whitlock, C., 1998. Paleoclimate simulations for North America over the past 21,000 years: features of the simulated climate and comparisons with paleoenvironmental data. *Quaternary Science Reviews* 17, 549–586.
- Bernabo, J.C., Webb III, T., 1977. Changing patterns in the Holocene pollen record of northeastern North America: a mapped summary. *Quaternary Research* 8, 64–96.
- Box, E.O., 1981. *Macroclimate and plant forms: an introduction to predictive modeling in phytogeography*. Tasks for Vegetation Science. Dr. W. Junk Publishers, Hauge.
- Bradshaw, R.H.W., Webb III, T., 1985. Relationships between contemporary pollen and vegetation data from Wisconsin and Michigan, USA. *Ecology* 66 (3), 721–737.
- Braun, E.L., 1950. *Deciduous Forests of Eastern North America*. Blakiston, New York, 596 pp.
- Broström, A., Coe, M., Harrison, S.P., Gallimore, R., Kutzbach, J.E., Foley, J., Prentice, I.C., Behling, P., 1998. Land surface feedbacks and palaeomonsoons in northern Africa. *Geophysical Research Letters* 25, 3615–3618.
- Cheddadi, R., Yu, G., Guiot, J., Harrison, S.P., Prentice, I.C., 1997. The climate of Europe 6000 years ago. *Climate Dynamics* 13, 1–9.
- Cheddadi, R., Lamb, H.F., Guiot, J., van der Kaars, S., 1998. Holocene climatic change in Morocco: a quantitative reconstruction from pollen data. *Climate Dynamics* 14, 883–890.
- Christensen, N.L., 2000. Vegetation of the southeastern coastal plain. In: Barbour, M.G., Billings, W.D. (Eds.), *North American Terrestrial Vegetation*, 2nd edn. Cambridge Univ. Press, Cambridge, UK, pp. 397–448.
- COHMAP Members, 1988. Climatic changes of the last 18,000 years: observations and model simulations. *Science* 24, 1043–1052.
- Cowling, S.A., 1999. Simulated effects of low atmospheric CO₂ on structure and composition of North American vegetation at the last glacial maximum. *Global Ecology and Biogeography Letters* 8, 81–93.
- Crosta, X., Pichon, J.-J., Burckle, L.H., 1998. Application of modern analog technique to marine Antarctic diatoms: reconstruc-

- tion of maximum sea-ice extent at the last glacial maximum. *Paleoceanography* 13, 284–297.
- Crowley, T.J., 1995. Ice age terrestrial carbon changes revisited. *Global Biogeochemical Cycles* 9, 377–389.
- Cushing, E.J., 1967. Late-Wisconsin pollen stratigraphy and the glacial sequence in Minnesota. In: Cushing, E.J., Wright Jr., H.E. (Eds.), *Quaternary Paleocology*. Yale Univ. Press, New Haven, pp. 59–88.
- Davis, M.B., 1976. Pleistocene biogeography of temperate deciduous forests. *Geoscience and Man* XIII, 13–26.
- Davis, O.K., 1995. Climate and vegetation patterns in surface samples from arid western USA: application to Holocene climatic reconstructions. *Palynology* 19, 95–117.
- DeFries, R., Hansen, M., Townshend, J.R.G., Sohlberg, R., 1998. Global land cover classifications at 8 km spatial resolution: the use of training data derived from Landsat imagery in decision tree classifiers. *International Journal of Remote Sensing* 19, 3141–3168.
- DeFries, R.S., Townshend, J.R.G., Hansen, M.C., 1999. Continuous fields of vegetation characteristics at the global scale at 1-km resolution. *Journal of Geophysical Research* 104 (D14), 16911–16923.
- DeFries, R.S., Hansen, M.C., Townshend, J.R.G., 2000. Global continuous fields of vegetation characteristics: a linear mixture model applied to multi-year 8 km AVHRR data. *International Journal of Remote Sensing* 21, 1389–1414.
- Delcourt, P.A., Delcourt, H.R., Webb III, T., 1984. Atlas of mapped distributions of dominance and modern pollen percentages for important tree taxa of eastern North America. *AASP Contributions Series*, vol. 14. American Association of Stratigraphic Palynologists Foundation, 131 pp.
- de Noblet, N.I., Prentice, I.C., Joussaume, S., Texier, D., Botta, A., Haxeltine, A., 1996. Possible role of atmosphere–biosphere interactions in triggering the last glaciation. *Geophysical Research Letters* 23, 3191–3194.
- Edwards, M.E., Anderson, P.M., Brubaker, L.B., Ager, T., Andreev, A.A., Bigelow, N.H., Cwynar, L.C., Eisner, W.R., Harrison, S.P., Hu, F.-S., Jolly, D., Lozhkin, A.V., McDonald, G.M., Mock, C.J., Ritchie, J.C., Sher, A.V., Spear, R.W., Williams, J.W., Yu, G., 2000. Pollen-based biomes for Beringia 18,000, 6000, and 0 ¹⁴C yr BP. *Journal of Biogeography* 27, 521–554.
- Elliott-Fisk, D.L., 2000. The taiga and boreal forest. In: Barbour, M.G., Billings, W.D. (Eds.), *North American Terrestrial Vegetation*, 2nd edn. Cambridge Univ. Press, Cambridge, UK.
- Fassnacht, K.S., Gower, S.T., MacKenzie, M.D., Nordheim, E.V., Lillesand, T.M., 1997. Estimating the leaf area index of north central Wisconsin forests using the landsat thematic mapper. *Remote Sensing of the Environment* 61, 229–245.
- Field, C.B., Randerson, J.T., Malmström, C.M., 1995. Global net primary production: combining ecology and remote sensing. *Remote Sensing of the Environment* 51, 74–88.
- Foley, J.A., Kutzbach, J.E., Coe, M.T., Levis, S., 1994. Feedbacks between climate and boreal forests during the Holocene epoch. *Nature* 371, 52–54.
- Foley, J.A., Levis, S., Prentice, I.C., Pollard, D., Thompson, S.L., 1998. Coupling dynamic models of climate and vegetation. *Global Change Biology* 4, 561–579.
- Gajewski, K., Vance, R., Sawada, M., Fung, I., Gignac, L.D., Halsey, L., John, J., Maisongrande, P., Mandell, P., Mudie, P.J., Richard, P.J.H., Sherin, A.G., Soroko, J., Vitt, D.H., 2000. The climate of North America and adjacent ocean waters ca. 6 ka. *Canadian Journal of Earth Sciences* 37, 661–681.
- Ganopolski, A., Kubatzki, C., Claussen, M., Brovkin, V., Petoukhov, V., 1998a. The influence of vegetation–atmosphere–ocean interaction on climate during the mid-Holocene. *Science* 280, 1916–1919.
- Ganopolski, A., Rahmstorf, S., Petoukhov, V., Claussen, M., 1998b. Simulation of modern and glacial climates with a coupled global model of intermediate complexity. *Nature* 391, 351–356.
- Goward, S.N., Dye, D.G., 1987. Evaluating North American net primary productivity with satellite observations. *Advances in Space Research* 7, 165–174.
- Guiot, J., 1990. Methodology of the last climatic cycle reconstruction in France from pollen data. *Palaeogeography, Palaeoclimatology, Palaeoecology* 80, 49–69.
- Guiot, J., Harrison, S.P., Prentice, I.C., 1993. Reconstruction of Holocene precipitation patterns in Europe using pollen and lake-level data. *Quaternary Research* 40, 139–149.
- Holdridge, L.R., 1967. *Life Zone Ecology* Tropical Science Center, Costa Rica.
- Houghton, R.A., 2001. Counting terrestrial sources and sinks of carbon. *Climatic Change* 48, 525–534.
- Hunt Jr, E.R., Piper, S.C., Nemani, R., Keeling, C.D., Otto, R.D., Running, S.W., 1996. Global net carbon storage exchange and intra-annual atmospheric CO₂ concentrations predicted by an ecosystem process model and three-dimensional atmospheric transport model. *Global Biogeochemical Cycles* 10, 431–456.
- Huntley, B., 1990. Dissimilarity mapping between fossil and contemporary pollen spectra in Europe for the past 13,000 years. *Quaternary Research* 33, 360–376.
- Huntley, B., 1996. Quaternary paleoecology and ecology. *Quaternary Science Reviews* 15, 591–606.
- Huntley, B., Birks, H.J.B., 1983. *An Atlas of Past and Present Pollen Maps for Europe: 0–13000 Years Ago*. Cambridge Univ. Press, Cambridge.
- Huntley, B., Prentice, I.C., 1988. July temperatures in Europe from pollen data, 6000 years before present. *Science* 241, 687–690.
- Jackson, S.T., 1990. Pollen source area and representation in small lakes of the northeastern United States. *Review of Palaeobotany and Palynology* 63, 53–76.
- Jackson, S.T., 1991. Pollen representation of vegetational patterns along an elevational gradient. *Journal of Vegetation Science* 2, 613–624.
- Jackson, S.T., Kearsley, J.B., 1998. Quantitative representation of local forest composition in forest-floor pollen assemblages. *Journal of Ecology* 86, 474–490.
- Jackson, S.T., Overpeck, J.T., 2000. Responses of plant populations and communities to environmental changes of the late Quaternary. *Paleobiology* 26, 194–220.
- Jackson, S.T., Webb, R.S., Anderson, K.H., Overpeck, J.T., Webb III, T., Williams, J.W., Hansen, B.C.S., 2000. Vegetation and environment in eastern North America during the last glacial maximum. *Quaternary Science Reviews* 19, 489–508.
- Joussaume, S., Taylor, K.E., 2000. The paleoclimate modeling in-

- tercomparison project. In: Braconnot, P. (Ed.), *Proceedings of the Third PMIP Workshop*. World Climate Research Programme, La Huardière, Canada, pp. 9–24.
- Kohfeld, K.E., Harrison, S.P., 2000. How well can we simulate past climates? Evaluating the models using global palaeoenvironmental datasets. *Quaternary Science Reviews* 19, 321–346.
- Kubatzki, C., Claussen, M., 1998. Simulation of the global biogeophysical interactions during the last glacial maximum. *Climate Dynamics* 14, 461–471.
- Kucharik, C.J., Foley, J.A., Delire, C., Fisher, V.A., Coe, M.T., Lenters, J.D., Young-Molling, C., Ramankutty, N., Norman, J.M., Gower, S.T., 2000. Testing the performance of a dynamic global ecosystem model: water balance, carbon balance, and vegetation structure. *Global Biogeochemical Cycles* 14, 795–825.
- Küchler, A.W., 1964. *Potential natural vegetation of the conterminous United States*. American Geographical Society Special Publication, vol. 36. Princeton Polychrome Press, New York, 116 pp.
- Kumar, M., Monteith, J.L., 1981. Remote sensing of crop growth. In: Smith, H. (Ed.), *Plants and the Daylight Spectrum*. Academic Press, San Diego, pp. 133–144.
- Kutzbach, J., Bonan, G., Foley, J., Harrison, S.P., 1996. Vegetation and soil feedbacks on the response of the African monsoon to orbital forcing in the early to middle Holocene. *Nature* 384, 623–626.
- Kutzbach, J.E., Gallimore, R., Harrison, S.P., Behling, P., Selin, R., Laarif, F., 1998. Climate and biome simulations for the past 21,000 years. *Quaternary Science Reviews* 17, 473–506.
- Levis, S., Foley, J., Pollard, D., 1999. CO₂, climate, and vegetation feedbacks at the last glacial maximum. *Journal of Geophysical Research* V104 (ND24), 31191–31198.
- Loveland, T.R., Reed, B.C., Brown, J.F., Ohlen, D.O., Zhu, J., Yang, L., Merchant, J.W., 2000. Development of a global land cover characteristics database and IGBP DISCover from 1-km AVHRR data. *International Journal of Remote Sensing* 21, 1303–1330.
- Matthews, E., 1983. Global vegetation and land use: new high resolution data bases for climate studies. *Journal of Climate and Applied Meteorology* 22, 474–487.
- Nemani, R.R., Running, S.W., 1995. Satellite monitoring of global land cover changes and their impact on climate. *Climate Change* 31, 395–413.
- Nemani, R.R., Running, S.W., 1996. Global vegetation cover changes from coarse resolution satellite data. *Journal of Geophysical Research* 101, 7145–7162.
- Olson, J.S., Watts, J.A., Allison, L.J., 1984. *Major World Ecosystem Complexes Ranked by Carbon in Live Vegetation: A Database*. Oak Ridge National Laboratory, Oak Ridge, 397 pp.
- Overpeck, J.T., Webb III, T., Prentice, I.C., 1985. Quantitative interpretation of fossil pollen spectra: dissimilarity coefficients and the method of modern analogs. *Quaternary Research* 23, 87–108.
- Overpeck, J.T., Webb, R.S., Webb III, T., 1992. Mapping eastern North American vegetation change of the past 18 ka: no-analogs and the future. *Geology* 20, 1071–1074.
- PALE Beringian Working Group, 1999. *Paleoenvironmental atlas of Beringia presented in electronic form*. *Quaternary Research* 52, 270–271.
- Peet, R.K., 2000. *Forests and meadows of the Rocky Mountains*. In: Barbour, M.G., Billings, W.D. (Eds.), *North American Terrestrial Vegetation*. Cambridge Univ. Press, Cambridge, UK.
- Petit, J.R., Jouzel, J., Raynaud, D., Barkov, N.I., Barnola, J.-M., Basile, I., Bender, M., Chappellaz, J., Davis, M., Delaygue, G., Delmotte, M., Kotlyakov, V.M., Legrand, M., Lipenkov, V.Y., Lorius, C., Pépin, L., Ritz, C., Saltzman, E., Stievenard, M., 1999. Climate and atmospheric history of the past 420,000 years from the Vostok ice core, Antarctica. *Nature* 399, 429–436.
- Peyron, O., Guiot, J., Cheddadi, R., Tarasov, P., Reille, M., de Beaulieu, J.-L., Bottema, S., Andrieu, V., 1998. Climatic reconstruction in Europe for 18,000 yr B.P. from pollen data. *Quaternary Research* 49, 183–196.
- Peyron, O., Jolly, D., Bonnefille, R., Vincens, A., Guiot, J., 2000. Climate of east Africa 6000 ¹⁴C yr. B.P. as inferred from pollen data. *Quaternary Research* 54, 90–101.
- Pflaumann, U., Duprat, J., Pujol, C., Labeysie, L.D., 1996. SIM-MAX: a modern analog technique to deduce Atlantic sea surface temperatures from planktonic foraminifera in deep-sea sediments. *Paleoceanography* 11, 15–35.
- Pielke Sr., R.A., Avissar, R., Raupach, M., Dolman, A.J., Zeng, X., Denning, A.S., 1998. Interactions between the atmosphere and terrestrial ecosystems: influence on weather and climate. *Global Change Biology* 4, 461–475.
- Prell, W.L., 1985. The stability of low-latitude sea-surface temperatures: an evaluation of the CLIMAP reconstruction with emphasis on the positive SST anomalies. TR025, US Department of Energy, Washington, DC.
- Prentice, I.C., 1985. Pollen representation, source area, and basin size: toward a unified theory of pollen analysis. *Quaternary Research* 23, 76–86.
- Prentice, I.C., 1988. Records of vegetation in time and space: the principles of pollen analysis. In: Huntley, B., Webb, T. (Eds.), *Vegetation History*. Handbook of Vegetation Science. Kluwer Academic Publishing, Dordrecht, pp. 17–42.
- Prentice, I.C., Webb III, T., 1998. BIOME 6000: reconstructing global mid-Holocene vegetation patterns from palaeoecological records. *Journal of Biogeography* 25, 997–1005.
- Prentice, I.C., Berglund, B.E., Olsson, T., 1987. Quantitative forest-composition sensing characteristics of pollen samples from Swedish lakes. *Boreas* 16, 43–54.
- Prentice, I.C., Bartlein, P.J., Webb III, T., 1991. Vegetation and climate changes in eastern North America since the last glacial maximum: a response to continuous climatic forcing. *Ecology* 72, 2038–2056.
- Prentice, I.C., Cramer, W., Harrison, S.P., Leemans, R., Monserud, R.A., Solomon, R.A., 1992. A global biome model based on plant physiology and dominance, soil properties and climate. *Journal of Biogeography* 19, 117–134.
- Prentice, I.C., Guiot, J., Huntley, B., Jolly, D., Cheddadi, R., 1996. Reconstructing biomes from palaeoecological data: a general method and its application to European pollen data at 0 and 6 ka. *Climate Dynamics* 12, 185–194.
- Prentice, I.C., Jolly, D., BIOME 6000 participants, 2000. *Mid-Hol-*

- ocene and glacial-maximum vegetation geography of the northern continents and Africa. *Journal of Biogeography* 27, 507–519.
- Rind, D., 1984. The influence of vegetation on the hydrologic cycle in a global climate model. In: Hansen, J.E., Takahashi, T. (Eds.), *Climate Processes and Climate Sensitivity*. AGU Geophysical Monograph. American Geophysical Union, Washington, DC, pp. 73–91.
- Ritchie, J.C., 1984. A Holocene pollen record of boreal forest history from the Travaillant lake area, lower Mackenzie River Basin. *Canadian Journal of Botany* 62, 1385–1392.
- Ritchie, J.C., 1987. *Postglacial Vegetation of Canada*. Cambridge Univ. Press, Cambridge, 178 pp.
- Rowe, J.S., 1972. *Forest regions of Canada*. 1300, Canadian Forestry Service, Department of Fisheries and the Environment, Ottawa.
- Sellers, P.J., Dickinson, R.E., Randall, D.A., Betts, A.K., Hall, F.G., Berry, J.A., Collatz, G.J., Denning, A.S., Mooney, H.A., Nobre, C.A., Sato, N., Field, C.B., Henderson-Sellers, A., 1997. Modelling the exchanges of energy, water, and carbon between continents and the atmosphere. *Science* 275, 502–509.
- Smith, T.M., Shugart, H.H., Woodward, F.I. (Eds.), 1997. *Plant Functional Types: Their Relevance to Ecosystem Properties and Global Change*. Cambridge Univ. Press, Cambridge, 369 pp.
- Snyder, J.P., 1982. *Map Projections Used by the U.S. Geological Survey*. Geological Survey Bulletin, vol. 1532. US Government Printing Office, Washington, DC, 313 pp.
- Sugita, S., 1994. Pollen representation of vegetation in Quaternary sediments: theory and method in patchy vegetation. *Journal of Ecology* 82, 881–897.
- Sugita, S., Gaillard, M.-J., Broström, A., 1999. Landscape openness and pollen records: a simulation approach. *The Holocene* 9, 409–421.
- Tarasov, P.E., Webb III, T., Andreev, A.A., Afanas'eva, N.B., Bezina, N.A., Bezusko, L.G., Blyakharachuk, T.A., Bolikhovskaya, N.S., Cheddadi, R., Chernavskaya, M.M., Chernova, G.M., Dorofeyuk, N.I., Dirksen, V.G., Elina, G.A., Filimonova, L.V., Glebov, F.Z., Guiot, J., Gunova, V.S., Harrison, S.P., Jolly, D., Khomutova, V.I., Kvavadze, E.V., Osipova, I.M., Panova, N.K., Prentice, I.C., Sarse, L., Sevastyanov, D.V., Volkova, V.S., Zernitskaya, V.P., 1998. Present-day and mid-Holocene biomes reconstructed from pollen and plant macrofossil data from the Former Soviet Union and Mongolia. *Journal of Biogeography* 25, 1029–1053.
- Texier, D., de Noblet, N., Harrison, S.P., Haxeltine, A., Joussaume, S., Jolly, D., Laarif, F., Prentice, I.C., Tarasov, P.E., 1997. Quantifying the role of biosphere-atmosphere feedbacks in climate change: a coupled model simulation for 6000 yr B.P. and comparison with palaeodata for northern Eurasia and northern Africa. *Climate Dynamics* 13, 865–881.
- Thompson, R.S., 1988. Glacial and Holocene vegetation history: western North America. In: Huntley, B., Webb, T. (Eds.), *Vegetation History*. Handbook of Vegetation Science. Kluwer Academic Publishing, Dordrecht, pp. 415–458.
- Thompson, R.S., Anderson, K.H., 2000. Biomes of western North America at 18,000, 6000 and 0 ¹⁴C yr BP reconstructed from pollen and packrat midden data. *Journal of Biogeography* 27, 555–584.
- Thunell, R., Anderson, D., Gellar, D., Miao, Q., 1994. Sea-surface temperature estimates for the tropical western Pacific during the last glaciation and their implications for the Pacific warm pool. *Quaternary Research* 41, 255–264.
- van Leeuwen, W.J.D., Huete, A.R., Walthall, C.L., Prince, S.D., Bégué, A., Roujean, J.L., 1997. Deconvolution of remotely sensed spectral mixtures for retrieval of LAI, fAPAR and soil brightness. *Journal of Hydrology* 188–189, 697–724.
- Waelbroeck, C., Labeyrie, L., Duplessy, J.-C., Guiot, J., Labracherie, M., Leclaire, H., Duprat, J., 1998. Improving past sea surface temperature estimates based on planktonic fossil faunas. *Paleoceanography* 13, 272–283.
- Watts, W.A., 1970. The full-glacial vegetation of northwestern Georgia. *Ecology* 51, 17–33.
- Watts, W.A., 1980. Late-Quaternary vegetation history at White Pond on the inner coastal plain of South Carolina. *Quaternary Research* 13, 187–199.
- Webb III, T., 1981. The past 11,000 years of vegetational change in eastern North America. *Bioscience* 31, 501–506.
- Webb III, T., 1986. Is vegetation in equilibrium with climate? How to interpret late-Quaternary pollen data. *Vegetation* 67, 75–91.
- Webb III, T., 1988. Glacial and Holocene vegetation history: eastern North America. In: Huntley, B., Webb, T. (Eds.), *Vegetation History*. Kluwer Academic Publishing, Dordrecht, pp. 385–414.
- Webb III, T., Kutzbach, J.E. 1998. An introduction to 'late Quaternary climates: data syntheses and model experiments'. *Quaternary Science Reviews* 17, 465–471.
- Webb III, T., Cushing, E.J., Wright Jr., H.E., 1983. Holocene changes in the vegetation of the midwest. In: Wright, H.E. (Ed.), *Late-Quaternary Environments of the United States*. University of Minnesota Press, Minneapolis, pp. 142–165.
- Webb III, T., Bartlein, P.J., Harrison, S.P., Anderson, K.H. 1993. Vegetation, lake levels, and climate in eastern North America for the past 18,000 years. In: Wright Jr., H.E., et al. (Eds.), *Global Climates Since the Last Glacial Maximum*, University of Minnesota Press, Minneapolis, MN, pp. 415–467.
- Whitehead, D.R., 1967. *Studies of full-glacial vegetation and climate in southeastern United States*. In: Cushing, E.J., Wright Jr., H.E. (Eds.), *Quaternary Paleocology*. Yale Univ. Press, New Haven, CT, USA, pp. 237–248.
- Williams, J.W., 2000. *Biome-Scale Vegetation Dynamics in North America since the Last Glacial Maximum: Maps and Reconstructions from Fossil Pollen Data and the Testing of Biogeography Models*. PhD Dissertation Thesis, Brown University, Providence, RI, 265 pp.
- Williams, J.W., Jackson, S.T., submitted for publication. Palynological and AVHRR observations of modern vegetational gradients in eastern North America.
- Williams, J.W., Bartlein, P.J., Webb III, T., 2000a. Data-model comparisons for eastern North America-inferred biomes and climate values from pollen data. In: Braconnot, P. (Ed.), *Proceedings of the Third PMIP Workshop*, 4–8 October 1999, Montreal, Canada, pp. 77–86.
- Williams, J.W., Webb III, T., Richard, P.J.H., Newby, P., 2000b. Late Quaternary biomes of Canada and the eastern United States. *Journal of Biogeography* 27, 585–607.
- Williams, J.W., Shuman, B.N., Webb III, T., 2001. No-analog con-

- ditions and rates of change in the vegetation and climate of eastern North America. *Ecology*.
- Williams, J.W., Shuman, B.N., Webb III, T., Leduc, P., Bartlein, P.J., in preparation. Vegetation dynamics at 1000-year intervals in northern and eastern North America since the Last Glacial Maximum.
- Woodward, F.I., 1987. Climate and plant distribution. Cambridge Studies in Ecology. Cambridge Univ. Press, Cambridge, 174 pp.
- Wright Jr., H.E., Kutzbach, J.E., Webb III, T., Ruddiman, W.F., Street-Perrott, F.A., Bartlein, P.J., 1993. Global Climates since the Last Glacial Maximum. University of Minnesota Press, Minneapolis, 569 pp.
- Yu, G., Chen, X., Ni, J., Cheddadi, R., Guiot, J., Han, H., Harrison, S.P., Huang, C., Ke, M., Kong, Z., Li, S., Li, W., Liew, P., Liu, G., Liu, J., Liu, Q., Liu, K.-B., Prentice, I.C., Qui, W., Ren, G., Song, C., Sugita, S., Sun, X., Tang, L., Van Campo, E., Xia, Y., Xu, Q., Yan, S., Yang, X., Zhao, J., Zheng, Z., 2000. Palaeovegetation of China: a pollen data-based synthesis for the mid-Holocene and last glacial maximum. *Journal of Biogeography* 27, 635–664.